

## Dry high speed milling of cobalt-base hard facing superalloy

M. Benghersallah\*, L. Boulanouar\*, G. Le Coz\*\*, A. Devillez\*\*, D. Dudzinski\*\*

\*Mechanical laboratory of Materials and Plant Maintenance (LR3MI), Mechanical Department of Engineering, University Badji Mokhtar BP12, Annaba 23000 Algeria, E-mail: Bengher\_moh@yahoo.fr

\*\*Laboratoire de Physique et Mécanique des Matériaux UMR CNRS 7554 ISCMP – Bâtiment C Ile du Saulcy 57045 METZ Cedex 01 France

**crossref** <http://dx.doi.org/10.5755/j01.mech.18.5.2707>

### 1. Introduction

In the competitive and open international market, quick response to business opportunity is considered as one of the important factors to ensure company competitiveness. New products must be more quickly and cheaply developed, manufactured and introduced to the market. The demand for shorter development and production times but also higher quality and greater efficiencies results in the emergence of rapid prototyping and rapid tooling techniques [1, 2].

The present study is a part of the project proposing a rapid tooling process for the forging industry. Dies are realised by metallic projection of refractory alloys on a substrate with a Plasma Transferred Arc system (PTA) [3-5], and finished by high speed milling.

Plasma Transferred Arc employs the plasma principle; plasma is a gas sufficiently ionized to be electrically conductive. In PTA, two DC power supplies are used to establish first a nontransferred arc (pilot arc) between a tungsten electrode and the anodic nozzle and then a transferred arc between the tungsten electrode and the workpiece. The pilot arc is struck by a High Frequency device and the plasma gas flowing around the cathode is ionized at the electrode tip, Fig. 1.

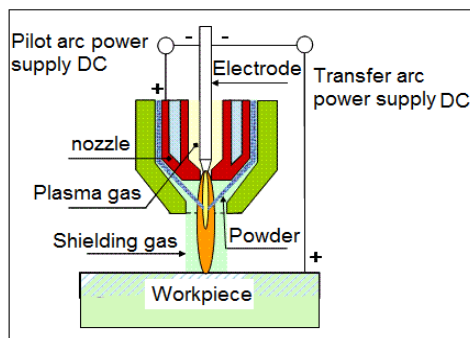


Fig. 1 Scheme of PTA deposition, from [4]

When the transferred arc is ignited, the workpiece becomes a part of the electrical circuit and the plasma arc is directed and focused into the workpiece. Metal powder is carried to the plasma jet by gas stream; the gas flow is also used to protect the metal from atmospheric contamination.

Hardfacing is a technique to restore the damaged dies, for example, to reusable condition. PTA is one of the most promising hardfacing processes; it leads to a homogeneous refined microstructure for the deposited thick layer, with low dilution and distortion in comparison with

other welding techniques, like Tungsten Inert Gas (TIG) or Metal Inert Gas (MIG) processes. In this study, PTA is proposed to be used as a rapid hard spray tooling process for forging dies.

Among the wide choice of metal powders for PTA deposition and hardfacing, Ni and Co-base alloys are commonly used. One group of the hardfacing alloys is known as 'Stellites', they are cobalt based alloys with high hardness at high temperature and high corrosion and wear resistance under high pressure conditions. The Co-Cr-W-C, Stellite 6 alloy is employed in the following study to realize the functional surfaces of a die for forging industry. However, after PTA deposition of Stellite 6, the deposited layers have to be machined to guarantee the surface roughness and to respect the geometrical tolerances of the functional surfaces.

The present work examines the machinability in dry conditions of deposited layers by PTA process. According to the high mechanical properties at elevated temperatures of the Stellite 6 alloy, the deposited layers are known to be very difficult to cut. Previous studies about high speed and dry machining of hardfacing [6-8] show that machinability is limited by a premature tool wear, and as a consequence by a reduced tool life, and additionally by surface integrity problems. The heat generation and the plastic deformation induced during machining affect the machined surface. The heat generated usually alters the microstructure of the alloy and induces residual stresses. Residual stresses are also produced by plastic deformation without heat. Heat and deformation generate cracks and microstructural changes, as well as large microhardness variations. Residual stresses have consequences on mechanical behaviour, especially on the fatigue life of the workpieces. Extreme care must be taken therefore to ensure the surface integrity during machining and to ensure adequate tool lives. Cutting conditions must be correctly defined and controlled. The major parameters to be controlled are: the choice of tool and coating materials, tool geometry, machining method, cutting speed, feed rate, and depth of cut. In addition, the machining process used in this study is milling, it is an intermittent operation. Tool cutting edge enters and exits from the workpiece several times per second producing cyclic heat and force loadings. In the milling operations, the end of tool life is more frequently limited by chipping, cracks and breakage of the tool cutting edge.

Different studies about machining performance of new cutting materials (cutting tool substrate and coatings) show that some significant improvement have been performed by the cutting tool manufacturers [9-15]; they give

bases for the milling and turning of difficult to cut materials [16-19].

Depending on machined material, mono or multi-layer CVD or PVD coatings on carbide insert may improve the cutting tool behaviour. When machining a new material, TiN coatings may be first choice and correspond to a reference. TiCN is an advanced coating with special properties, among the PVD coatings it has the lowest friction coefficient. It has high impact resistance, but its use is limited to low cutting temperatures, until 400°C. It adheres particularly well to the carbide substrate, so it may be used as the first layer. Al<sub>2</sub>O<sub>3</sub> coating is a good choice when chemical stability and cratering wear resistance is researched. TiAlN is presently the high performance multi-layer coating used for High Speed Milling (HSM). It presents the hardness of 90 HRC and oxidation temperature of 815°C [20]. AlTiN coating has been recently developed for dry or minimum quantity lubrication high speed machining. Its properties are excellent adhesion, fine grained structure and very smooth surface [17].

## 2. Experimental procedure

### 2.1. Worked materials

The worked material is Stellite 6 alloy deposited on blocks of 55NCDV7 steel using the PTA process. Monolayer and bilayer PTA depositions were performed. The hardfacing surface presents some irregularities; grooves are visible on Fig. 2. Some inhomogeneities, small cavities and cracks are observed in the thickness of the deposited layer. In comparison with the imperfections introduced by the MIG hardfacing process, these defects are greatly reduced.

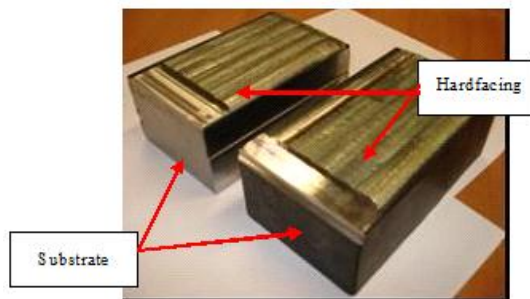


Fig. 2 Test parts

Microhardness tests have been performed from top of the deposited surface to the substrate, the results are presented on Fig. 3, PTA and MIG hardfacing process are compared. For the monolayer PTA hardfacing, the hardness varies greatly from 750 HV at the top of the surface to 500 HV near the neighbouring of the substrate interface. For the MIG hardfacing, the hardness remains approxi-

mately constant at the value of 400 HV. The large dependence of micro-hardness with depth observed after PTA hardfacing was also obtained after laser deposition of NiAl+ZrO<sub>2</sub> on Ti-6Al-4V, C. K. Shaa and al. [15, 21-22].

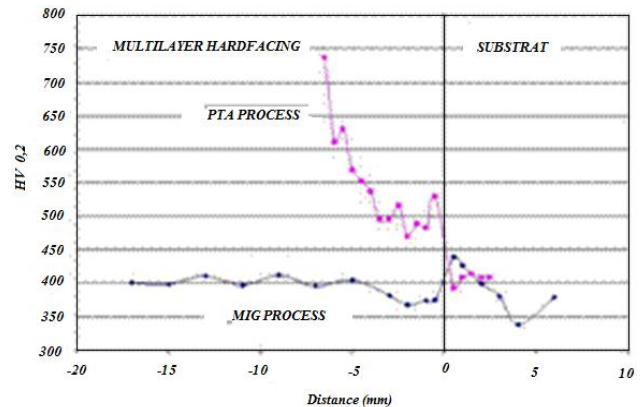


Fig. 3 Hardness comparison for Stellite 6 hardfacing with MIG and PTA processes

### 2.2. High speed milling machine

Machining tests were realised on a High Speed Machine Rödgers RP600 instrumented with power controllers Wattpilot™ developed by the society DIGITAL WAY. These controllers allow to record the spindle and the feed motors power consumptions. Power controllers are usually employed to monitor the tool wear and tool breakage. In opposition to piezo-electric dynamometer they are not limited in force.

### 2.3 Cutting tool and milling method

Down milling operations were performed, the cutting tool was an end mill of 16 mm diameter with two carbide inserts Sandvik Coromant R390 by different coatings and presented on Fig. 4.

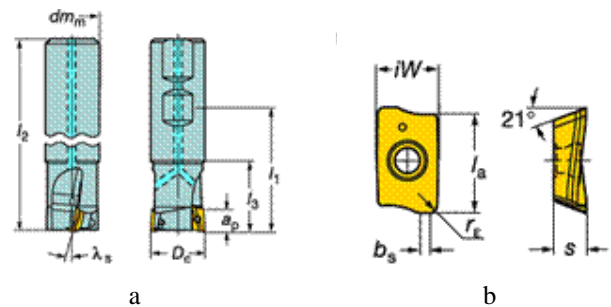


Fig. 4 a) Milling cutter and b) Insert geometry

The five commercial coatings were used on carbide compositions are referenced Table 1.

Table 1

Commercial coating carbide inserts

Insert	Substrate	Coating	Coating process
C1	Fine grain Bicarbite Rich in cobalt	Multilayer TiN	PVD
C2	Fine grain Bicarbite High toughness	Multilayer TiN+TiCN+TiAlN	PVD
C3	Fine grain Bicarbite Rich in cobalt	Multilayer TiN+ TiCN+Al <sub>2</sub> O <sub>3</sub>	CVD
C4	Fine grain Bicarbite Rich in cobalt	Multilayer TiN+ TiCN	PVD
C5	Middle grain carbide	AlTiN nanocrystalline	PVD

Series of tests

N° of test	$V_c$ , m/min	$f_z$ , mm/d	$N$ , tr/min	$A$ , mm/min	$a_e$ , mm	$a_p$ , mm	Hardfacing
1	190	0.067	3800	512	0.3	3	monolayer
2	190	0.067	3800	512	0.3	5	bilayer
3	230	0.067	4600	650	0.3	5	bilayer
4	120	0.067	2400	321	0.3	5	bilayer

The multilayer coatings used for the C1, C2, C3, C4, inserts are coatings with TiN, TiCN and  $Al_2O_3$  layers deposited by PVD or CVD process have an average thickness of 2 to 3  $\mu m$ . The hardness of the coating varies from 2000 to 3000 HV. For the C5 insert, the coating nanocrystalline multilayer AlTiN has a total thickness of 2  $\mu m$ , the hardness is 3500 HV

### 2.3. Milling tests

For all tests the cutting length was 100 mm, the radial width  $a_e$  was 0.3 mm and the feed rate  $f_z$  was chosen equal to 0.067 mm/tooth. In the first series of tests the cutting speed was constant and equal to 190 m/min; the objective was to compare the inserts compoment on the monolayer hardfacing, comparing wear and power consumption, Table 2.

The best inserts are qualified for the second cutting test on the bilayer hardfacing, to determinate the appropriate cutting speeds, Table 2.

Between two cuttings, the offset is the distance  $a_e$ . Cutting depth  $a_p$  is defined to machine only the hardfacing. Substrate stays intact.

### 2.4. Tool wears observation

To discuss about the tool wear phenomenon, it is necessary to observe, to measure and to quantify it. Two machines are used:

1. The optical microscope TESA and it software TESA VISIO is used to observe the tool wear evolution along the cutting tests this permits to determinate the tool life. The qualification criterion is the degradation of the tetragonal insertions. Classically, in industry, it is considered that acuity tool is degraded after a clearance wear of 0.3 mm [23]. This criterion is used to determinate the test end.

2. A Veeco NT1100 (Wyko®) Optical Profiler, using the white light interferometry technique presented by Devillez et al [24] is employed to monitor cutting parameters and to generate 3D images of the wear patterns of the cutting tools. This technique was also used with the same objectives by Dawson and Kurfess [25-27].

## 3. Results and discussion

### 3.1. Power signal exploitation

All power controllers have been activated during the test. Electrical power consumed by x, y, z and spindle axes engines have been recorded and treated. Calibration of Roders power transducer is not finished, so power can't be converted into force [28]. So, the work is based on power signal. Spindle power signal is extremely interfered

for lower cutting speed (120 and 190 m/min) as showed on Fig. 5. When the power increases, the noise disappears. Thus, the signal could be used, as shown on Fig. 6.

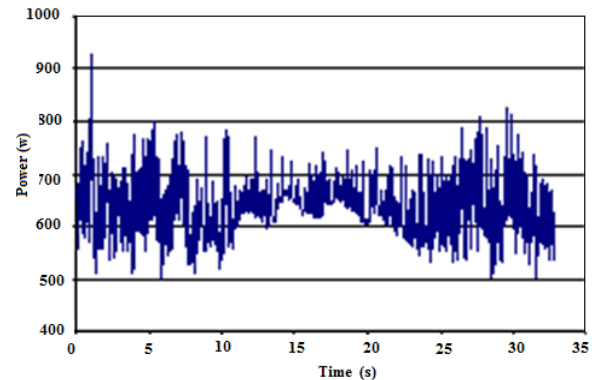


Fig. 5 Spindle power signal ( $V_c = 120$  m/min)

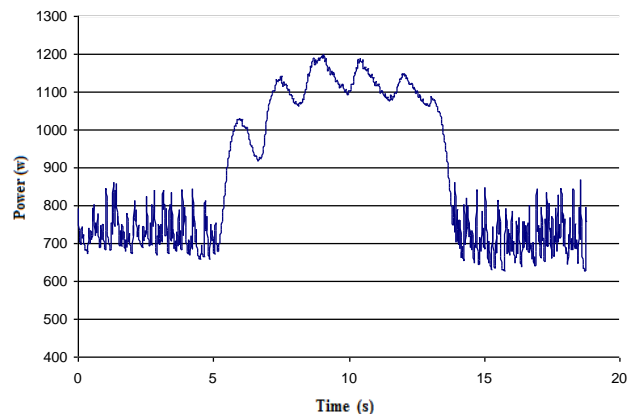


Fig. 6 Spindle power signal ( $V_c = 230$  m/min)

X and Y axes signals, as on Figs. 7 and 8, are more distinct but variation of cutting depth is not visible. Power variations exist but can't be really identify.

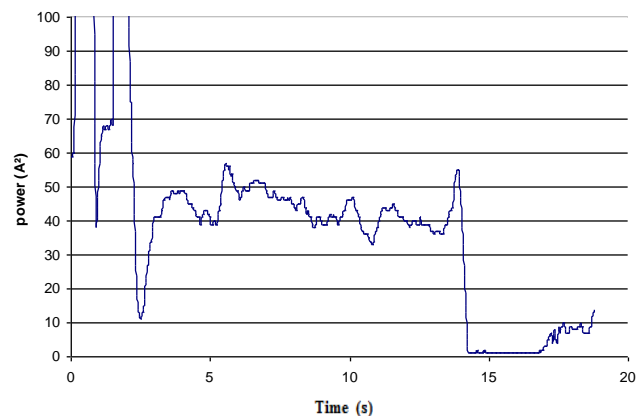


Fig. 7 X axis power ( $V_c = 230$  m/min)

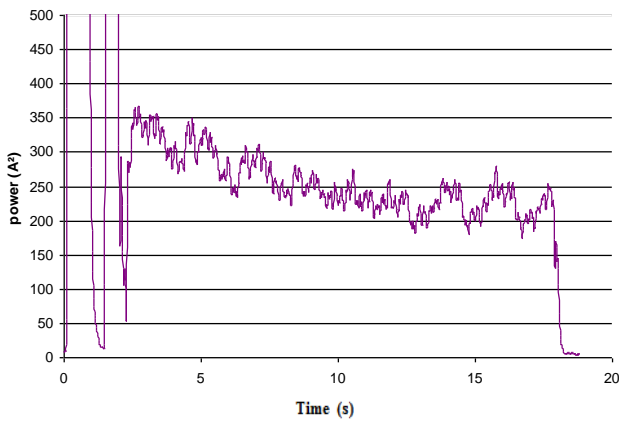


Fig. 8 Y axis power ( $V_c = 230$  m/min)

Z axis power value will be the signal used. The signal is distinct and stable for every inserts and every cutting speeds. This signal, shown on Fig. 9, allows to see power variations during a cutting cycle. Thus, the irregular shape of PTA hardfacing appears. This signal also allows to see the evolution between two cutting cycles.

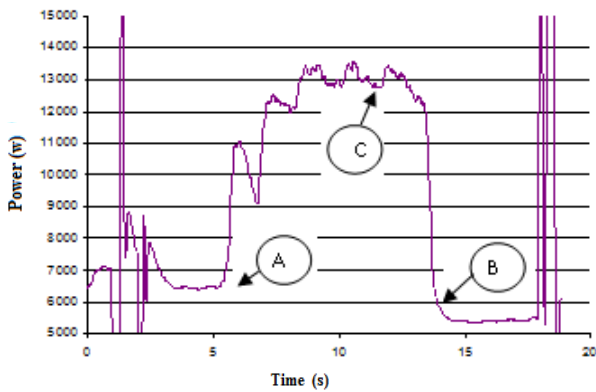


Fig. 9 Z axis power ( $V_c = 120$  m/min)

The curve is characterised by high power before 5 and after 30 seconds, linked to the vertical spindle movements. Machining starts at the 6th second (A) and finishes at the 14th (B). The six hardfacing beads are visible on power curve. All power measurements of the study are strictly taken in the same stable conditions, on last but one hardfacing bead (C).

### 3.2. Study of monolayer hardfacing machinability with $V_c = 190$ m/min, test 1

The first machining test of monolayer PTA permits to classify five different tools to qualify the best ones. Cutting conditions used are precised Table 2.

The analysis of power curves on Fig. 10 shows that from the 5 tools nuances tested, C2 and C5 consume less power than other ones. The analysis of wear curves on Fig. 11 shows that flank wear is fast for C3, C1 and C4, exceeding quickly the admissible wear of 0.3 mm. Contrary to, C2 and C5, VB is less than 0.3 mm.

The inserts observation by optical and interferometric microscope shows that for every cutting tool, the flank wear increases continuously with a notch effect, followed by major chipping on the cutting face. The cutting edge loses its acuity. Little by little, the coating is pulled out and wear occurs in the substrate. This phenome-

non is particularly at the insert area in contact with the top part of the hardfacing, at 3 mm of the nose, see Figs. 12, a and 12, b. Interferometric analysis of the cutting and flank face for the different inserts shows that after the coating dismissed (thick layer of 6 to 7  $\mu\text{m}$ ), the flank wear is not so important in depth and notch is localised at 3 mm of the nose, and there is no crater on the cutting face, only chipping, see Fig. 12, c. This means a great cohesion of the micrograins carbide substrate. The exception is made for the C1 insert, Fig. 12, d, which presents a major degradation all along its cutting edge.

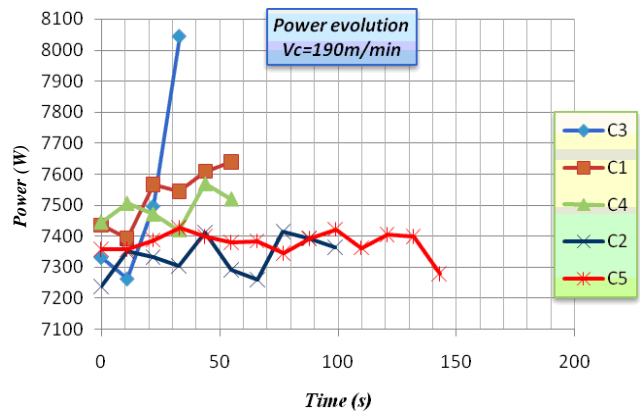


Fig. 10 Power consumption for five testing inserts  $V_c = 190$  m/min monolayer hardfacing

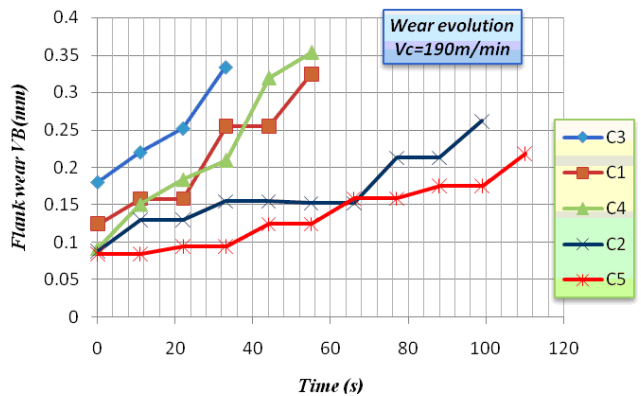


Fig. 11 Wear evolution for five testing inserts

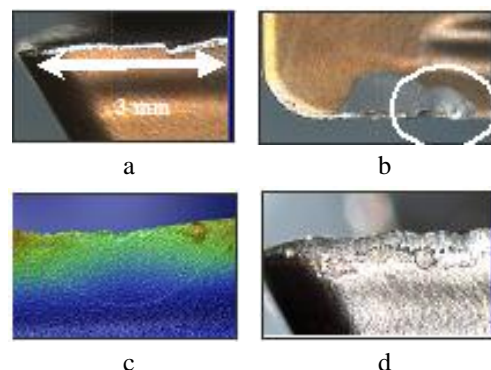


Fig. 12 Different types of wear obtained by (a), (b), (d) optical microscope and (c) interferometric microscope

Comparing power consumed and wear, only inserts C2 and C5 are kept to the next of the study, and to resume:

- for grade C2 insert, the flank wear is slowed down and cutting face chipping is important;
- for grade C5 insert, the flank wear is slowed down too and seems to be braked. The cutting edge keeps it acuity but a large chipping is on the cutting face driving to the test end.

3.3. Study of bilayer hardfacing machinability with  $V_c = 190$  m/min, test 2

The second test is performed in a bilayer hardfacing. Thus, the cutting depth is higher. The cutting conditions are precised Table 2.

C2 and C5 inserts have given some satisfaction results, comparatively to milling tests on the monolayer hardfacing, especially for insert C5. The analysis of power curves on Fig. 13 shows that power for C2 is really unstable. Contrary to, C5 insert the power variation is quite stable and decreases at the test end. Power consumption of C2 insert is globally higher than C5 insert. Analysis of wear curves on Fig. 14 shows that the flank wears evolution is regular for the two inserts and C5 tool wear is slower. This wear resistance is due to the protection of the Al-TiN nanocrystalline coating. However, when the coating is pulled out by the chafing and the chip adhesion, the middle grains substrate presents a remarkable weakness compared to the micrograins substrate of the insert C2. The cutting face chipping of the C2 insert is well operated and there is a resistance to the chipping area propagation. Then, it is the flank wear, see Fig. 14 which causes the test stop, by a maximal wear superior of the limit. This wear is the highest at 5 mm of the nose and, as for the first test, this phenomenon is particularly presented on the insert part in contact with the top part of the hardfacing, see Figs. 15, a and b.

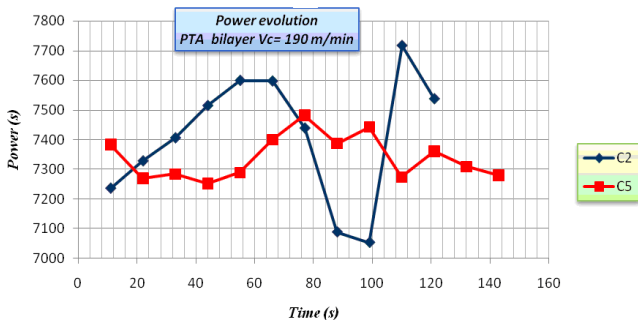


Fig. 13 Power consumption for C2 and C5 testing inserts  $V_c = 190$  m/min bilayer hardfacing

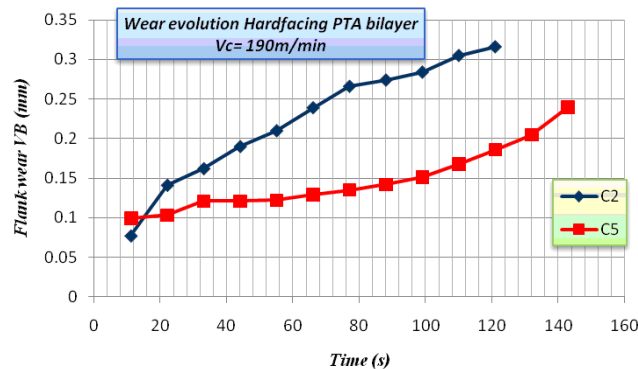


Fig. 14 Wear evolution C2 and C5 testing inserts  $V_c = 190$  m/min bilayer hardfacing

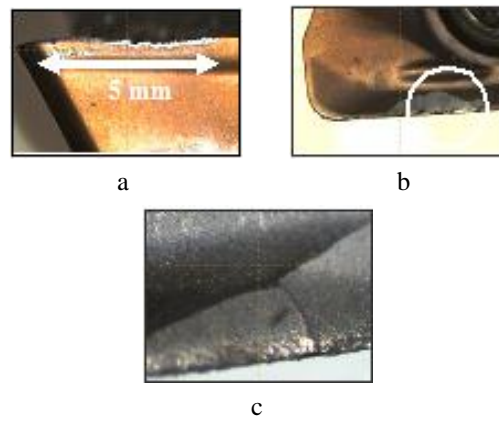


Fig. 15 Types of wear for (a), (b) C2 insert and (c) C5 insert

The examination of the tool wear by white light interferometer, see Fig. 16, a, shows that the flank of the C2 insert presents an important wear with a deep notch. A chipping is making on the cutting face and there is a loose of the cutting edge acuity. The interferometric picture of the cutting insert C5 shows a coating pulling out, see Fig. 16, b, and a substrate crack on the cutting face, verified Fig. 15, c, which conduces to the test end. C5 tool has a better wear resistance but the crack shows it dangerousness after the coating pulled out.

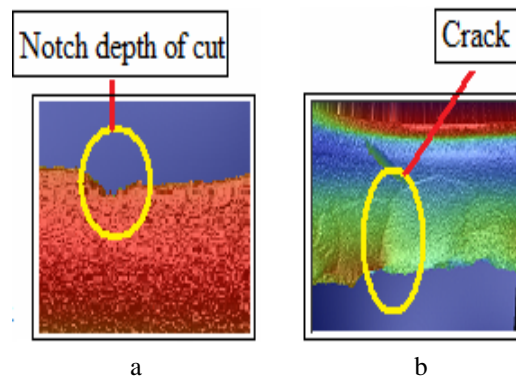


Fig. 16 Interferometric picture of (a) C2 cutting edge and (b) C5 cutting face

3.4. Study of bilayer hardfacing machinability with  $V_c = 230$  m/min, test 3

The third machining tests series, which cutting conditions are presented Table 2, shows, as on Fig. 17 that the power is generally continuously increasing during the test, except for insert C5. During the first 20 seconds, and after the 60th second, the power decreases. It may be the result of the running in of the insert for the first case, equally observed on Fig. 9, A. Another hypothesis is a chip adhesion phenomenon which can modify the geometry of the cutting edge and the cutting angle. Then, the power can be various but the general tendency is a power increase. Analysis of wear curves on Fig. 18 shows that insert C2 wears faster and loses its performances compare to insert C5 which have a better wear resistance, even the higher cutting speed.

Examination of insert C2 by the optical microscope, Fig. 19, reveals, again, on the cutting face near the cutting edge, a severe chipping and a sufficient flank wear

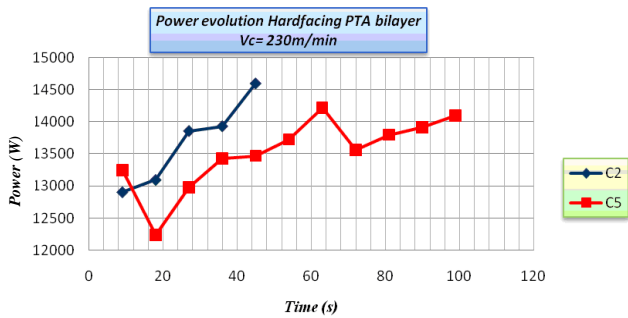


Fig. 17 Power consumption for C2 and C5 testing inserts  $V_c = 230$  m/min bilayer hardfacing

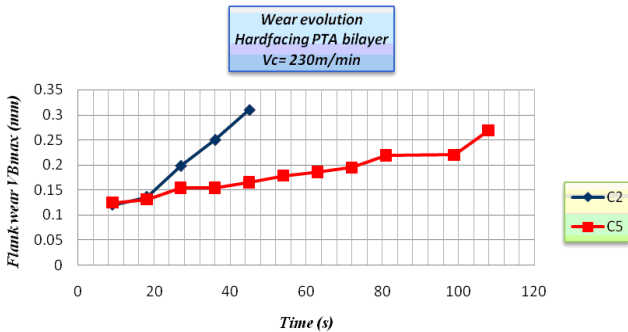


Fig. 18 Wear evolution C2 and C5 testing inserts  $V_c = 230$  m/min bilayer hardfacing

to stop the test. For insert C5, the exam has shown that flank wear evolution is slow and especially the cutting edge keeps its acuity. Chipping on the cutting face is also the same that for the other conditions ( $V_c = 190$  m/min), and a notch starts at 5 mm of the nose, where the area is the most solicited.



Fig. 19 Cutting edge chipping localisation

3.5. Study of bilayer hardfacing machinability with  $V_c = 120$  m/min, test 4

A lower cutting speed is tested for the test 4 with a  $V_c$  of 120 m/min. Cutting condition are also précised in Table 2.

The third machining test has given satisfaction and equivalent results for the two inserts. Analysis of power curves on Fig. 20 shows that power consumption increases during the test. As on Figs. 13 and 17, power consumed by C5 tool, decreases during the first cutting of the test. Now, C2 has best performance in term of power consumption. Wear curves of Fig. 21 show that the two inserts have a good comportment during the test. Insert C2 wear is progressive. For insert C5, the wear is made by stages: the first one after 50 seconds and the second one after 240 seconds.

Examination with microscope, Fig. 22, shows that the two inserts present chipping on the cutting faces, at 5 mm of the nose. It is important to notice that the cutting

speed affects the ration chipping wear/flank wear. The less the cutting speed, the most the flank wear is, compare to the chipping wear.

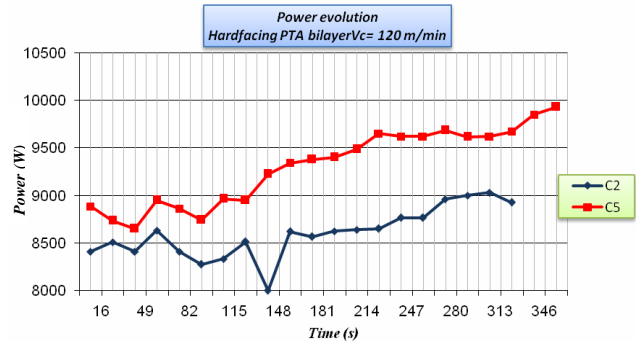


Fig. 20 Power consumption for C2 and C5 testing inserts,  $V_c = 120$  m/min bilayer hardfacing

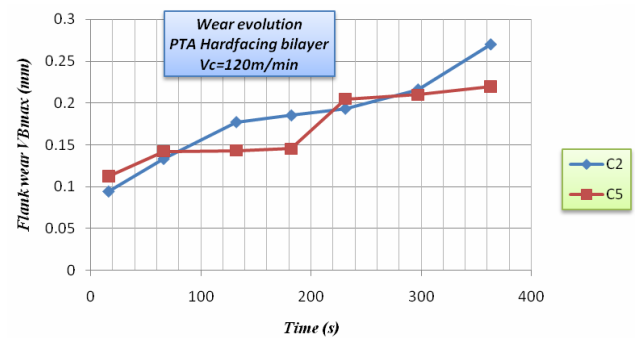


Fig. 21 Wear evolution C2 and C5 testing inserts  $V_c = 120$  m/min bilayer hardfacing

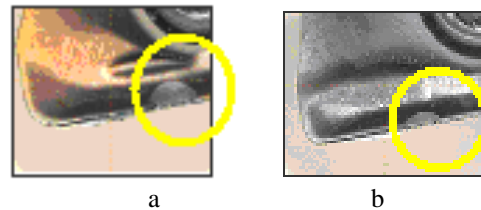


Fig. 22 Chipping on the cutting faces (a) C2 and (b) C5

3.6. Cutting speed  $V_c$  and identification of Taylor law parameters

Different cutting speeds have been tested during the bilayer hardfacing study, all on the same conditions ( $a_p$ ,  $a_e$  and material). Thus, it is possible to determinate the appropriate cutting speed, comparing power. That one which consumes the less is that one which limits cutting forces. Points used to draw the graph of Fig. 23 correspond to the power values at test start (1st pass). For tool C2 and C5 awarded, the appropriated speed is  $V_c = 190$  m/min, but in term of power.

To determinate the appropriate cutting speed, it also necessary to consider the wear evolution. It is possible to generalise the wear evolution function of cutting speed using the Taylor law  $V_c = T^G \times C$ ; with  $T$  the tool life (min),  $V_c$  the cutting speed (m/min) and  $C$  and  $G$  constants depending of the machined material and the cutting tool [26-27, 29]. With the experimental values obtained, the constants are identified. Thus, the law for this machining with C5 insert became

$$V_c = T^{0.5} \times 2186 \quad (1)$$

and for C2 insert became

$$V_c = T^{0.31} \times 645 \quad (2)$$

Thus, for a cutting speed of 80 m/min, the tool life would be respectively 746 and 839 seconds, see Fig. 24, and C2 insert would be the more efficient. But for a higher speed than 190 m/min, the tendency is inversed. So, the coating C5 shows its superiority, in term of tool life, for the high speed cutting of hard metal parts in dry condition.

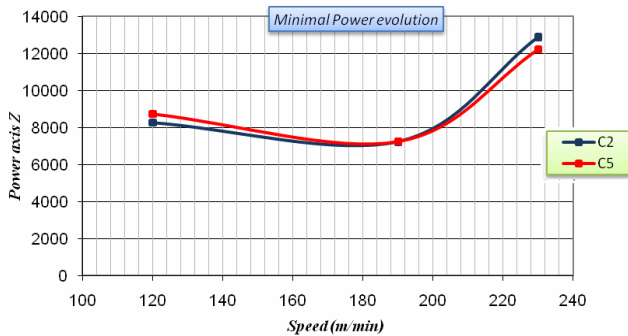


Fig. 23 Power evolution function of cutting speed

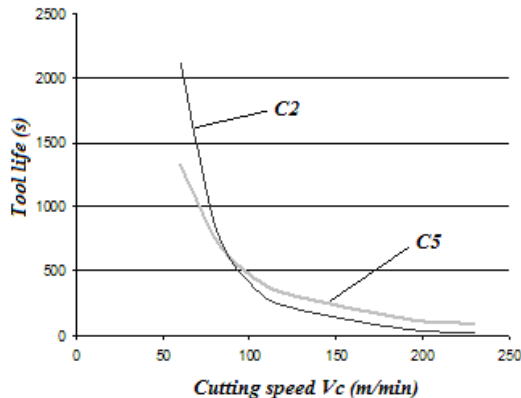


Fig. 24 Taylor law application

#### 4. Conclusions and future prospect

The experimental study permits to conclude about the machinability of a PTA hardfacing layers of Stellite 6. It is hard but possible. The responsible of the major wear is the 1 mm superior layer of the hardfacing (700 HV0.2) which conduces to notch and cutting face chipping. Thus, the cutting inserts for milling have different kinds of wears: progressive wear of the flank face characterised by notch of the part in contact with the hardfacing top part; and severe chipping in the cutting face. Also, during the high speed machining of hard metals characterised by hard machinability, it is recommended to reduce the admissible flank wear criteria  $V_{bmax}$  to  $[V_b] = 0.2$  mm. The chipping, by its length and its depth can be another criteria to consider. The experiment allows to say that the most appropriate cutting speed in term of cutting forces is 190 m/min but with the cutting speed of 80 m/min, the tool life starts to be acceptable. Moreover, the coating C5 is the most efficient with high speed and dry cutting conditions. Practically, the study has confirmed that the implementation of the Wattpi-

lote system to the Rödgers RP600 for the machining control is efficient. It gives the opportunity to follow the evolution of the cutting process in term of power. Power curves of X, Y and especially Z axes are in phase with the wear curves. The power improving during the milling process is probably linked to the tool wear. Theoretically, it is possible to follow and to control the inserts wear with the power help.

The methodology adopted for the tests and the criteria considered to quantify the parameters integrated in the process give a qualification of the tool without uncertainty. Thus, two inserts have been awarded with the aim of industrial applications and the coating C5 has proved its particular effectiveness for hard metal machining.

The future prospects can be resumed to solve the problem of fast coating pull out of the cutting face, it is necessary to develop, on another study, the phenomenon of chip adhesion and the coating properties. Thus, a local lubrication on the cutting face by air blow mixed with a freeze and lubricant properties liquid could improve the results.

In parallel of the study, the hardfacing by Stellite 21 with PTA process has been realized. Its hardness is low, near of 500 HV0.2. Stellite 6 machining conclusions could be applied to this new hardfacing. To complete the study of the Stellite 6 hardfacing, a measurement of the residual stresses in the milling part is programmed. Finally, to complete the study, other coatings must be tested.

#### Acknowledgements

We would like to thank the ANR, French National Research Agency, for its financial support for this study and more generally for supporting the PROMETFOR project.

#### References

1. Akula, S.; Karunakaran, K.P. 2006. Hybrid adaptive layer manufacturing: An Intelligent art of direct metal rapid tooling process, *Robotic and Computer Integrated Manufacturing* 22(2): 113-123. <http://dx.doi.org/10.1016/j.rcim.2005.02.006>.
2. Song, J.L.; Li, Y.T.; Deng, Q.L.; Hu, D.J. 2007. Rapid prototyping manufacturing of silica sand patterns based on selective laser sintering, *Journal of Materials Processing Technology* 187-188: 614-618. <http://dx.doi.org/10.1016/j.jmatprotec.2006.11.108>.
3. Gatto, A.; Bassoli, E.; Fornari, M. 2004. Plasma Transferred Arc deposition of powdered high performance alloys: process parameters optimisation as a function of alloy and geometrical configuration, *Surface and Coatings Technology* 187(2-3): 265-271. <http://dx.doi.org/10.1016/j.surfcoat.2004.02.013>.
4. [www.plasmateam.com](http://www.plasmateam.com).
5. D'Olivera, A.S.C.M.; Paredes, R.S.C.; Santos, R.L.C. 2006. Pulsed current plasma transferred arc hardfacing, *Journal of Materials Processing Technology* 171: 167-174. <http://dx.doi.org/10.1016/j.jmatprotec.2005.02.269>.
6. Fouilland, L.; Iordache, L.; El Mansori, M.; Huguet, A. 2005. Caractérisation métallurgique des couches de rechargement base-Cobalt par soudage de matrice à chaud: influence des paramètres d'élaboration, *Matériaux et Techniques* 93: 163-169. <http://dx.doi.org/10.1051/mattech:2005005>.

7. **Sidhu, T.S.; Prakash, S.; Agrawal, R.D.** 2006. Studies of the metallurgical and mechanical properties of high velocity oxy-fuel sprayed stellite-6 coatings on Ni- and Fe-based superalloys, *Surface and Coatings Technology* 201(1-2): 273-281.  
<http://dx.doi.org/10.1016/j.surfcoat.2005.11.108>.
8. **EL Mansori, M.; Nouari, M.** 2007. Dry machinability of nickel-based weld-hardfacing layers for hot tooling, *International Journal of Machine Tools & Manufacture* 47: 1715-1727.  
<http://dx.doi.org/10.1016/j.ijmachtools.2006.12.007>.
9. **El Mansori, M.; Fouillard-Paillé, L.; Pierron, F.** 2005. Usinabilité à grande vitesse et à sec des couches du rechargement base-nickel par soudage d'outillage à chaud, *Mécanique & Industries* 6: 211-225.  
<http://dx.doi.org/10.1051/meca:2005022>.
10. **Rena, X.J.; Yang, Q.X.; James, R.D.; Wang, L.** 2004. Cutting temperatures in hard turning chromium hardfacings with PCBN tooling, *Journal of Materials Processing Technology* 147: 38-44.  
<http://dx.doi.org/10.1016/j.jmatprotec.2003.10.013>.
11. **CETIM** 1996. Les atouts de l'usinage à grande vitesse: Fraisage et perçage des métaux durs.
12. **Aslan, E.** 2004. Experimental investigation of cutting tool performance in high speed cutting of hardened X210Cr12 cold-work tool steel (62HRC), *Material and Design*.
13. **Nordin, M.; Sundstrom, R.; Selinder, T.I.; Hogmark, S.** 2000. Wear and failure mechanisms of multilayered PVD TiN TaN coated tools when milling austenitic stainless steel, *Surface and Coatings Technology* 133-134: 240-246.  
[http://dx.doi.org/10.1016/S0257-8972\(00\)00933-6](http://dx.doi.org/10.1016/S0257-8972(00)00933-6).
14. **Nordin, M.; Larsson, M.; Hogmark, S.** 1998. Mechanical and tribological properties of multilayered PVD TiN/CrN, TiN/MoN, TiN/NbN, TiN/TaN coating on cemented carbide, *Surface and Coatings Technology* 106: 234-241.  
[http://dx.doi.org/10.1016/S0257-8972\(98\)00544-1](http://dx.doi.org/10.1016/S0257-8972(98)00544-1).
15. **Boutin, Y.** 2005. L'usinage à Grande Vitesse, les matériaux de coupe, *Sup-métal*, février.
16. **Camuscu, N.; Aslan, E.** 2005. A comparative study on cutting tool performance in end milling of AISI D3 tool steel, *Materials Processing Technology* Avril 2005.
17. **Haron, C.H.; Ginting, A.; Arshad, H.** 2007. Performance of alloyed uncoated and CVD-coated carbide tools in dry milling of titanium alloy Ti-6242S, *Journal of Materials Processing Technology* 185: 77-82.  
<http://dx.doi.org/10.1016/j.jmatprotec.2006.03.135>.
18. **Devillez, A.; Schneider, F.; Dominiak, S.; Dudzinski, D.; Larrouquere, D.** 2005. Cutting forces and wear in dry machining of Inconel 718 with coated carbide tools, *Wear* 262: 931-942.  
<http://dx.doi.org/10.1016/j.wear.2006.10.009>.
19. **Arndt, M.; Kacsich, T.** 2003. Performance of new AlTiN coatings in dry and high speed cutting, *Surface Coating Technology* 163/164: 674-680.  
[http://dx.doi.org/10.1016/S0257-8972\(02\)00694-1](http://dx.doi.org/10.1016/S0257-8972(02)00694-1).
20. **Endrino, J.L.; Fox-Rabinovich, G.S.; Gey, C.** 2006. Hard AlTiN, AlCrN PVD coatings for machining of austenitic stainless steel, *Surface Coating Technology* 200(24): 6840-6845.  
<http://dx.doi.org/10.1016/j.surfcoat.2005.10.030>.
21. **Ghani, J.A.; Choudhury, I.A.; Hassan, H.** 2004. Application of Taguchi method in the optimization of end milling parameters, *Materials Processing Technology* 145: 84-92.  
[http://dx.doi.org/10.1016/S0924-0136\(03\)00865-3](http://dx.doi.org/10.1016/S0924-0136(03)00865-3).
22. **Shaa, C.K.; Lin, J.C.; Tsai, H.L.** 2003. The impact characteristics of Ti-6Al-4V plates hardfacing by laser alloying NiAl + ZrO<sub>2</sub> powder, *Journal of Materials Processing Technology* 140: 197-202.  
[http://dx.doi.org/10.1016/S0924-0136\(03\)00713-1](http://dx.doi.org/10.1016/S0924-0136(03)00713-1).
23. **Kim, T.Y.; Kim, J.** 1996. Adaptive cutting force control for a machining center by using indirect cutting force measurement, *Int. J. Mach. Tools Manufact.* 36(8): 925-937.  
[http://dx.doi.org/10.1016/0890-6955\(96\)00097-1](http://dx.doi.org/10.1016/0890-6955(96)00097-1).
24. **Balkrishna, C.R.; Shin, Y.C.** 1999. A comprehensive dynamic cutting force model for chatter prediction in turning, *International Journal of Machine Tools & Manufacture* 39: 1631-1654.  
[http://dx.doi.org/10.1016/S0890-6955\(99\)00007-3](http://dx.doi.org/10.1016/S0890-6955(99)00007-3).
25. **Fox-Rabinovich, G.S.; Endrino, J.L.; Beake, B.D.; Kovalev, A.I.; Veldhuis, S.C.; Ning, L.; Fontaine, F.; Gray, A.** 2006. Impact of annealing on microstructure, properties and cutting performance of an AlTiN coating, *Surface & Coatings Technology* 201: 3524-3529.  
<http://dx.doi.org/10.1016/j.surfcoat.2006.08.075>.
26. **Devillez, A.; Lesko, S.; Mozer, W.** 2004. Cutting tool crater wear measurement with white light interferometry, *Wear* 256(1-2): 56-65.  
[http://dx.doi.org/10.1016/S0043-1648\(03\)00384-3](http://dx.doi.org/10.1016/S0043-1648(03)00384-3).
27. **Dawson, T.G.; Kurfess, T.R.** 2005. Quantification of tool wear using white light interferometry and three-dimensional computational metrology, *International Journal of Machine Tools and Manufacture*, 45(4-5): 591-596.  
<http://dx.doi.org/10.1016/j.ijmachtools.2004.08.022>.
28. **Kim, T.Y.; Woo, J.; Shin, D.; Kim, J.** 1999. Indirect cutting force measurement in multi-axis simultaneous NC milling processes, *International Journal of Machine Tools & Manufacture* 39: 1717-1731.  
[http://dx.doi.org/10.1016/S0890-6955\(99\)00027-9](http://dx.doi.org/10.1016/S0890-6955(99)00027-9).
29. **Marksberry, P.W.; Jawahir, I.S.** 2007. A comprehensive tool-wear / tool-life performance model in the evaluation of NDM (near dry machining) for sustainable manufacturing, *International Journal of Machine Tools & Manufacture*.



M. Benghersallah, L. Boulanouar, G. Le Coz, A. Devillez,  
D. Dudzinski

KARŠČIUI ATSPARAUS KOBALTO KIETLYDINIO  
PAVIRŠIAUS SAUSASIS FREZAVIMAS DIDELIU  
GREIČIU

Re z i u m ė

Štampuojant naudojami stiprūs smūgiai, didelės jėgos, įtempiai ir temperatūros, todėl matricos turi būti ypač atsparios. Projekto, remiamo Prancūzijos nacionalinės agentūros (ANR) PROMETFOR, tikslas – sukurti greitą, štapavimo sąlygas atitinkantį prototipų procesą, kurį būtų galima integruoti į „Satellite 6“ paviršiaus padengimo kietlydiniu programos plazminio apvirinimo procesą. Nagrinėjamas kietlydinio paviršiaus sausasis apdirbimas naudojant du apdirbimo įrankius ir didelio greičio frezavimo stakles su naudojamos galios įrašymo įtaisu „Wattpilote“. Tyrimo tikslas – parodyti kietlydinio apdirbimą, optiniu mikroskopu ir dienos šviesos interferometru matuojant galią ir įvorių išsidėvėjimą, taikant įvairias strategijas ir esant įvairioms pjovimo sąlygoms.

M. Benghersallah, L. Boulanouar, G. Le Coz, A. Devillez,  
D. Dudzinski

DRY HIGH SPEED MILLING OF COBALT-BASE  
HARD FACING SUPERALLOY

S u m m a r y

The forging work involves extreme impacts, forces, stresses and temperatures. Thus, mould dies must be extremely resistant. The aim of the project PROMETFOR, supported by the French National Agency (ANR), is to perform a rapid prototyping process answering to forging conditions integrating a Stellite 6 hardfacing deposited by a PTA process. This study talks about the dry machining of the hardfacing, using a two inserts machining tool and a high speed milling machine equipped by a power consumption recorder Wattpilote. The aim is to show the machinability of the hardfacing, measuring the power and the insert wear by optical microscope and white light interferometer, using different strategies and cutting conditions.

**Keywords:** Stellite 6, Plasma Transferred Arc (PTA) deposition, Dry machining, tool wear, tool coatings.

Received June 01, 2011  
Accepted October 19, 2012